PROCEEDINGS OF ECOS 2023 - THE 36TH INTERNATIONAL CONFERENCE ON
EFFICIENCY, COST, OPTIMIZATION, SIMULATION AND ENVIRONMENTAL IMPACT OF ENERGY SYSTEMS
25-30 JUNE, 2023, LAS PALMAS DE GRAN CANARIA, SPAIN

An Investigation of the Synthesis and Optical Properties of a Novel Ag/ZnO Hybrid Nanofluid for Spectral Splitting in Photovoltaic-Thermal Systems

Sandesh S. Chougule[a], Gaurav G. Bolegave[b], Bhaskar Soni[c], Chandan Pandey[a], Vinayak Kamble[b] and Christos N. Markides[a]

[a] Clean Energy Processes (CEP) Laboratory, Department of Chemical Engineering, Imperial College London, London SW72AZ, United Kingdom,
[b] School of Physics, Indian Institute of Science Education and Research, Thiruvananthapuram, Kerala 695551, India,
[c] Department of Physics, Faculty of Science, The Maharaja Sayajirao University of Baroda, Vadodara, Gujrat 390002, India,
[*] Corresponding author: s.chougule@imperial.ac.uk

Abstract:

The deficient utilisation of the solar spectrum in conventional hybrid concentrating photovoltaic-thermal (CPV-T) technologies leads to a detrimental decrease in PV efficiency due to elevated temperatures. Solar spectral beam splitting (SBS) is an advancement in PV-T system design, which aims to use the full solar spectrum with minimal optical losses. The implementation of fluid-based SBS designs is economically feasible, with optical features that can be tuned by selecting suitable nanofluids with a desired concentration. Fluid-based SBS filters are advantageous over other filters for PV-T systems due to their ability to operate simultaneously as thermal storage as well as heat transfer media in these systems. In the present study, we report on the optical and thermophysical properties of a novel water-based Ag-ZnO hybrid nanofluid. The filter is synthesised by adding Ag to ZnO nanoparticles by a wet chemical method for improved stability. Silver (Ag) allows visible light harvesting (down conversion of UV to the visible region of the solar spectrum) and good optical properties in the visible and near-IR regions. An Ag shell can be embedded into the core of zinc oxide (ZnO) nanoparticles for improved stability. The presence of ZnO enables excellent optical properties, including high visible transmittance and high UV absorption. The presence of structural defects in ZnO induces colour centres which are deep traps emitting in the visible. Ag-ZnO nanofluids with different nanoparticle concentrations were tested to measure absorbance and transmittance using UV spectroscopy. These nanofluid filters can be used for full spectrum utilisation (by SBS) which helps in achieving: (i) down conversion in the UV region, (ii) transmit visible and near IR (NIR) region (desired wavelength of Si PV cell optoelectronic efficiency) ,and (iii) absorb (filter) the IR region of the solar spectrum (for downstream thermal use/applications).

Keywords:

CPV-T; Colour Centres; Light Harvesting; Nanofluid; Solar Spectral Beam Splitting.

1. Introduction

In the 21st century, the energy crisis and climate change are both among the most pressing global issues. Fossil fuels derived from carbon are responsible for both problems. In the future, energy demand will undoubtedly increase, so how to balance energy supply and CO2 emissions will become a global concern. In this case, it's essential to focus on emerging technologies involving new energies and decarbonization. As one of the most important renewable energy sources, solar power could play a crucial role in solving the energy crisis and cutting down on pollution. It may be utilised in two important ways, namely through direct production of electricity via photovoltaic conversion (PV) and through the conversion of heat i.e. photothermal (PT) conversion. Solar photovoltaic panels use only a small fraction of the solar spectrum for the generation of charge carriers, while the remainder causes undesirable heating of the panels, reducing their efficiency [1]. A hybrid photovoltaic-thermal (PV-T) system was therefore proposed in which the heat generated by the PVs is dissipated by a heat exchanger fluid, commonly called a coolant, thus resulting in a PV-T hybrid system [2]. The hybrid system is also more energy-efficient than individual photovoltaic or thermal systems. The performance of PV-Ts has improved significantly with the emergence of alternative heat exchange fluids

https://doi.org/10.52202/069564-0158

[3]. However, the emerging spectral splitting PV-T technology can produce greater fluid temperature and higher total efficiencies by separating the PV and thermal units.

In the spectral splitting method, the part of sunlight that cannot be converted into electricity is filtered out before it reaches the PV cells. Solar radiation is split into ultraviolet (UV), visible, and infrared (IR) spectrums by this technique, which requires matching the spectral bands of the cells and the wavelengths absorbed by the filter. A solar PV system uses the visible spectrum to produce electricity, while UV and IR spectra are absorbed and collected elsewhere as heat. It has been reported in previous studies that fluid-based spectral beam splitters (SBS) are more efficient than other kinds of splitters, such as interference filters and holographic filters [4]. Furthermore, fluid based SBS can be implemented economically, and its filtering features can be easily altered by choosing suitable by varying fluid properties. The fluid-based filter is also advantageous over other filters for PV-T systems since it can simultaneously serve as a thermal storage medium and a heat transfer medium. There have been experimental studies conducted with water as a filter for PV-T collectors in the past. Water is a common liquid, used conventionally in such systems and has excellent thermal and optical properties. There has been evidence that water improves the performance of PV-T, and many researchers have explored the ability of traditional fluids to absorb solar irradiance not effectively utilised by PV cells [4,5], including water, inorganic salts, glycols, and oils. Pure fluids can only absorb a portion of the infrared light, while they perform poorly in the UV region of the solar spectrum, so PV-T systems with pure fluid filters are inefficient.

Water-based nanofluids have been recommended by many studies as beam splitters in PV-T systems [6,7]. PV modules will heat up unnecessarily when they are exposed to wavelengths that are outside of their spectral ranges, thereby reducing efficiency. Nanofluids may solve the challenges discussed above because of their tunable optical properties. A nanofluid comprises a stable suspension of nanoparticles in a base fluid (e.g., water). In addition, nanoparticles allow the splitter to adjust its bandwidth and absorption peak continuously according to the amount of bandgap energy needed for converting solar energy into electricity [8]. Several experimental studies have so far investigated the performance of nanofluid filtered PV-T systems. This led to an ideal nanofluid filter for a particular solar cell [4, 5]. An interesting method for improving nanofluid beam splitting involves plasmonic metal nanomaterials. Plasmonic nanoparticles that manipulate, guide, and localise the incident light. Silver (Ag) is among the most important metals for plasmonic particles, it has demonstrated capabilities for visible light harvesting [9] as well as support in the visible and near-infrared spectrum. A silver nanofluid is highly effective in both thermal and electrical conversions in previous studies involving beam splitting applications such as- Silver nanoparticles are also highly suitable for industrialization and commercialisation. Zhang et al. [10] conducted an indoor experiment to optimise the heat/electricity production of a PV-T system filtered by Ag/water nanofluid. The results confirmed that arranging the nanofluid above PV modules is beneficial for heat collection and cell temperature regulation. The performance of a PV-T system with nanofluid filter consisting of silver-silica nanoplates as visible light absorbers and silica-coated gold and gold-copper nanorods as infrared absorbers was evaluated through an indoor test [9]. The results showed that the c-Si PV cells based PV-T system with Ag-SiO2 nanofluids achieved the highest combined efficiency of 40%, while the electrical efficiency was only 6%. Han et al. [11] developed a high-performance optical filter using water-based Ag-CoSO4 nanofluid for SBS PV/T systems. The measured transmittance indicated that water-based Ag-CoSO4 nanofluid is superior to Ag/water nanofluid in terms of performance. A PV-T system with water based rGO-Ag nanofluid filters was experimentally investigated by Abdelrazik et al. [12]. As a result of the experimental results, the proposed system showed better performance than a PV system with only PV cells, and the electrical efficiency was generally less than 10%, whereas the thermal efficiency ranged between 24-30%. Despite these advantages, the readily oxidising nature of silver in air restricts its use. This drawback may be overcome by embedding Ag nanoparticles into stable oxides such as zinc oxide (ZnO). As an optoelectronic material, ZnO exhibits excellent optical properties like transmittance, suggesting the possibility of using it with Ag nanoparticles [13,14].

This work presents plasmonic silver metal with ZnO nanoparticles, made using simple wet chemical methods. The hybrid material has excellent spectral splitting properties that can be used in PVs to harvest visible light and convert it into electrical power. The narrow bandwidth of transparency (400-1000 nm) also leads to heat absorption by filtering UV and infrared rays. The water-based Ag-ZnO nanofluids has been assessed with optical transmission measurements, whereas Ag-ZnO hybrid nanomaterials is examined about structure, morphology, and chemical composition, which helps confirm the observed optical properties with those of the material. The preliminary results reported could be useful in providing a better insight in the optical and thermal processes that leads to SBS. Localised surface plasmons of Ag nanostructures are observed in the visible region (400 nm), ZnO band edge absorption is observed above 375 nm, and IR absorption, particularly for low-energy photons, is observed. More work is required for selection of the nanofluid filter parameters, including nanoparticle type, size, mass fraction, base fluid type, etc. Nevertheless, the results are promising to demonstrate a spectral beam splitting with environment friendly, benign and economical composition.

2. Experimental details

2.1. Materials

Zinc nitrate hexahydrate [$Zn(NO_3)_2.6H_2O$, mol. wt. = 297.49 g/mol, 99.99% pure, from Sigma Aldrich], Silver nitrate [$AgNO_3$, mol. wt. = 169.87 g/mol, 99.90% pure, from Sigma Aldrich], PVA [mol. wt. = 96800 g/mol, degree of polymerization = 2000, from Fischer Scientific], ammonia solution (NH_4OH, conc. 25%, from Merck), and sucrose ($C_{12}H_{22}O_{11}$, mol. wt. = 342.30 g/mol, 99.95% pure, from Merck) were used for the synthesis of ZnO -Ag hybrid nanoparticles.

2.2. Synthesis method

The process of synthesis of *Ag coated ZnO hybrid nanoparticles* has been shown in Fig 1. There were two main stages in the synthesis procedure of ZnO:Ag nanoparticles. In the first stage, Zn^{2+}-PVA-sucrose precursor powders were created by a chemical reaction between aqueous solutions of Zn^{2+} salt and PVA-sucrose polymer, as described in reference [15–18]. The next step involved further processing the precursor powders to create ZnO:Ag core-shell nanoparticles. A comprehensive explanation is given below.

In synthesis, 1:10 mass ratio of PVA and sucrose was mixed in water at reaction temperature of 60–65 ^oC with continuous magnetic stirring to disperse 0.2 M aqueous Zn^{2+} salt solution. The PVA-sucrose used in this process acts as a surfactant and offers a stable medium for the nanoparticles'-controlled growth through encapsulation in polymer micelles [19,20]. The sucrose additive improves the average viscosity of the reaction solution. It was noted that in the solution, the salts had an endothermic reaction with the PVA-sucrose molecules. By adding NH_4OH solution in the required quantity to support the hydrogenation of Zn^{2+} ions in the reaction solution, the pH of the mixed solution was maintained at 9 throughout the reaction. Following the reaction, the mixture was cooled to room temperature and aged at 20-25 °C for 24 hours before the transparent, colourless top layer of PVA-sucrose was decanted out. To obtain the fluffy, voluminous, whitish mass of polymer capped precursor powders, the obtained precipitate was dried at a controlled temperature of 50–60 °C after being washed with methanol to remove any unreacted residual PVA–sucrose. After pulverising the polymer precursor powders in a mortar and pestle, they were heated for two hours at 400–600 °C to produce refined ZnO nanoparticles. The final size of the particles is largely controlled by the heat treatment temperature.

In the next step, 5.0 g of the dried ZnO precursor powders were mixed with 100 ml of a 0.25 M solution of $AgNO_3$ in water. This was done in the dark at 60 °C under constant stirring. After about 30 minutes of reaction time at this temperature, the powders were recovered by decanting the $AgNO_3$ solution, washing them at least twice in hot water, and then drying them under low pressure (10 to 100 mbar) at 25 °C. The dried powders were then heated for 2 hours in ambient air at 500 °C. Followed by recrystallization, the ZnO nanoparticles are encapsulated by a stable, thin layer of Ag.

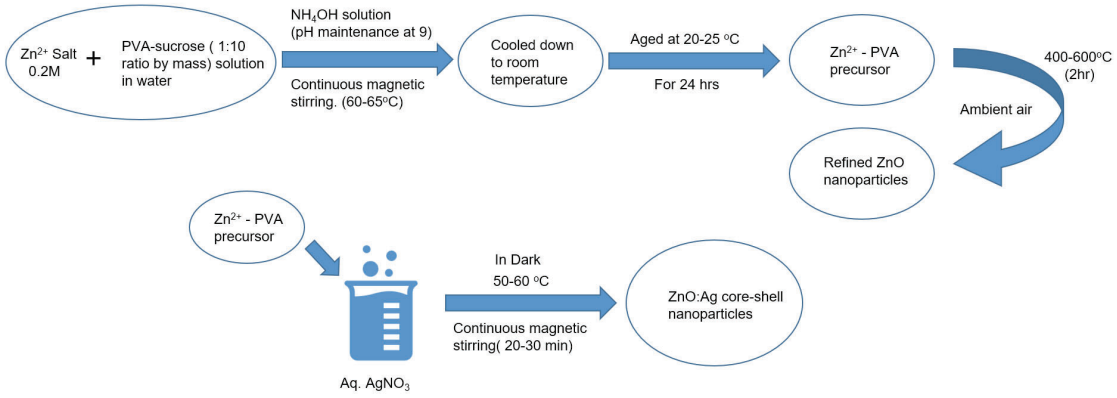

Figure 1. *Synthesis route of Ag coated ZnO hybrid nanoparticles.*

2.3. Characterisation

The crystalline nature and structure of synthesised Ag coated ZnO hybrid nanoparticles was examined under Bruker D8 powder X-ray diffractometer using Cu K_α source of radiation wavelength 1.5406 °A in the range 5 ° to 90 ° with a step size of 0.02 °. The particle morphology and elemental composition of the samples was analysed using FEI Nova Nanosem 450 Field Emission SEM equipped with Energy Dispersive X-ray spectroscopy (EDS). The individual particle morphology was investigated with FEI Tecnai G2 sprit Bio-Twin TEM at an accelerated voltage of 120 kV. To probe at the local structures of the chosen regions under investigation, an in-situ study of electron diffraction from selected areas (SAED) and high-resolution TEM imaging was carried out with FEI Tecnai G2 F30 S-Twin TEM at an accelerated voltage of 300 kV. The Raman spectra were captured on a Horiba Jobin

https://doi.org/10.52202/069564-0158

Vyon LabRam HR Raman by exciting with a 532 nm laser at room temperature. The optical transmittance spectra of the sample were taken in aqueous solution at room temperature with Perkin Elmer Lambda 950. The sample was sonicated for 30 minutes for well dispersion of nanoparticles in water. ZnO:Ag/Water nanofluids of mass fractions 50 ppm, 30 ppm, 15 ppm, and 5 ppm were made. Transmittance and absorption spectra were taken in the cuvette of 10 mm optical length.

3. Results and discussion

Figure 2 (a) shows the XRD pattern of the as-prepared ZnO-Ag sample. The pattern shows broad and distinct peaks which marks the nanocrystalline nature of the sample. The pattern is indexed to the hexagonal wurtzite type (space group P63mc) crystal structure of ZnO [JCPDS card # 036-1451]. Three distinct peaks corresponding to metallic silver of face-centred-cubic (fcc) crystal structure [JCPDS card # 04-0783] have been identified. The same have been marked as Ag with given (*hkl*) indices. The peaks are sufficiently broad in either case, which denotes the small particle size.

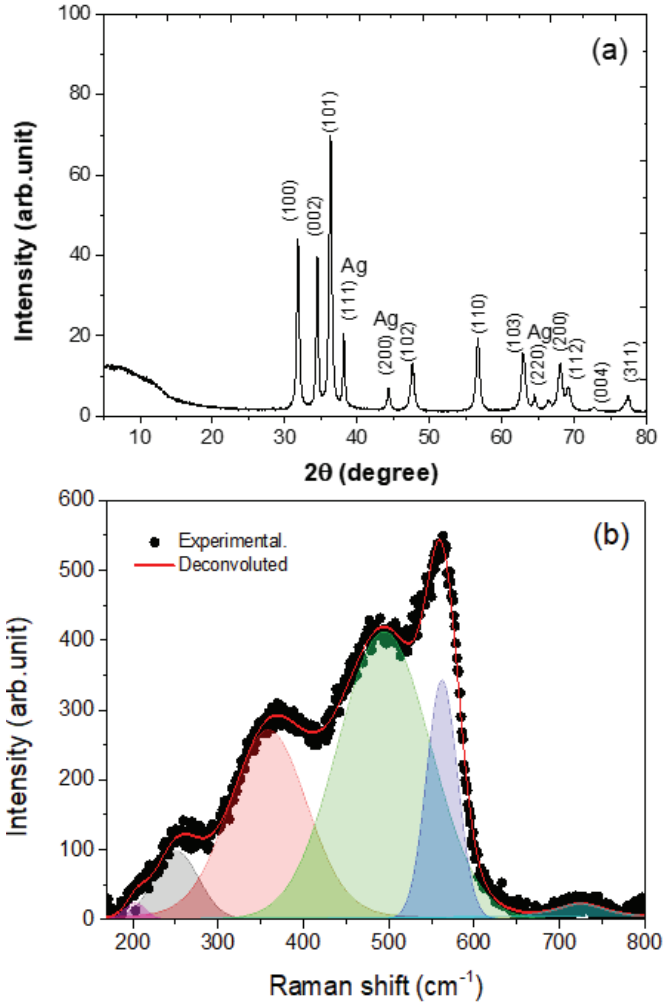

Figure 2. *(a) X-ray diffraction patterns, and (b) room temperature Raman spectrum of Ag-ZnO hybrids.*

The room temperature Raman spectra of Ag-ZnO as shown in Figure 2(b). The spectrum shows five distinct peaks that are listed in Table 1 along with their probable assignments [21–23]. Overall, from the comparison of observed data with that of reported literature, it can be observed that the Raman modes are significantly broadened in the present sample and the usual high intense peak of 438 cm^{-1} $E_{2(high)}$ is suppressed and the 563.2 cm^{-1} peak is observed to rise which is often ascribed to either high oxygen defects, substitutional impurities [21] or even lower particle sizes. [22] In this case, the smaller crystallite size along with presence of Ag additives may have resulted into such highly dispersive Raman absorption bands.

Table 1. Comparison of observed Raman peaks and probable modes reported in literature.

Peak position (cm^{-1})	Probable mode
205.1	2 $E_{2(low)}$ at 210 cm^{-1}
252.8	Not found
357.3	$E_{2(high)}$-$E_{2(low)}$ at ~340 cm-1 and E1(TO) at ~380 cm^{-1}
493.9	$E_{2(high)}$ at 440 cm^{-1}
563.2	A_1(low optical) or E_1 (low optical)) at 576 cm^{-1}

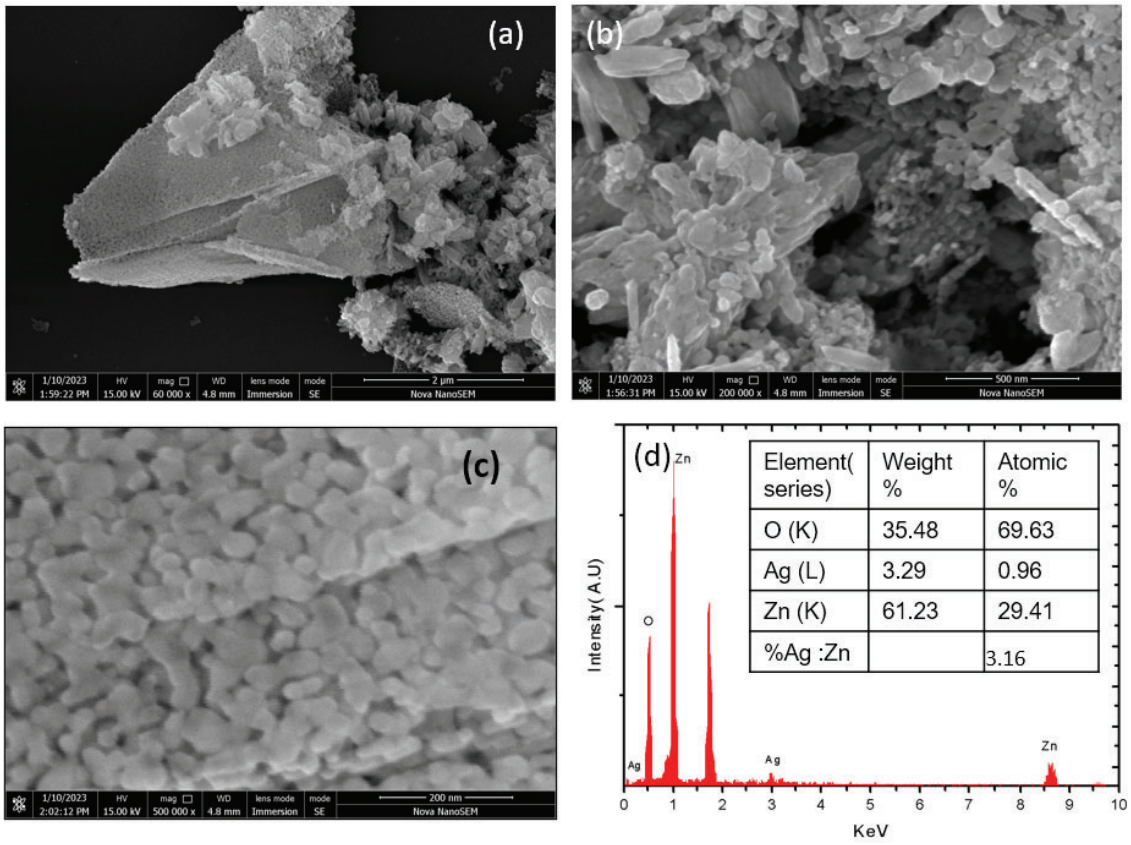

Figure 3. *Scanning electron micrographs of Ag-ZnO hybrid at: (a) low ,and (b, c) high magnifications showing the nanoscale particles (~50 nm). (d) energy dispersive spectrum of the Ag-ZnO sample with the quantification shown inset.*

Figure 3 shows the FESEM images of Ag-ZnO hybrid nanoparticles synthesised at 500 °C after heating the precursor for 2h in air. The loose agglomerates can be seen in the micrographs of the sample (Figure 3 a, b). In the particle clusters, a magnified view (Figure 3. b) reveals particles arranged in petal-like structures. Figure 3(d) depicts the elemental composition of the Ag-ZnO nanoparticles obtained at 500 °C. The presence of Zn, O, and Ag elements is confirmed in the samples, according to the EDS spectrum. The quantitative analysis indicates that Zn and Ag elements have atomic contents of 29.41%, and 0.96%, respectively.

Figure 4 shows the typical TEM images (a-d) and HRTEM (e) of Ag-ZnO nanoparticles. Figure 4 shows well dispersed particles. The average particle size was calculated from a histogram shown in Figure 4(f) and it is found to be 25–30 nm, with a narrow size distribution (±20 nm). The high-resolution TEM (HRTEM) image of a single particle is shown in Figure 4(e) it reveals that the particles may have facets with regular shape which gives them a thickness contrast. Nevertheless, the hexagonal shape is evident from Figure 4(a) also. The visible lattice reflections are close to an interplanar spacing of 0.27 nm (as shown in Figure 4 (e)). The results demonstrate the Ag along with ZnO nanoparticles. A typical selected area electron diffraction pattern (SAED) of nanoparticles is provided in Figure 4(g). It is made up of ZnO and Ag lattices that look like separate, concentric rings with spots in between. There are six characteristic rings of d_{hkl} values 0.2851 nm, 0.2503 nm, 0.1938 nm, 0.1659 nm, 0.1503 nm, and 0.1394 nm that correspond to the (100), (101), (102), (110), (103), and (112) planes of ZnO respectively, and the two characteristic rings of d_{hkl} values 0.2099 nm and 0.1112 nm correspond to the (200) and (222) planes of Ag. The d_{hkl} values derived from the SAED pattern and those

https://doi.org/10.52202/069564-0158

derived from the X-ray diffractograms are in close agreement. Due to the lower intensity of the diffraction spots, some reflections of ZnO and Ag could not be distinguished.

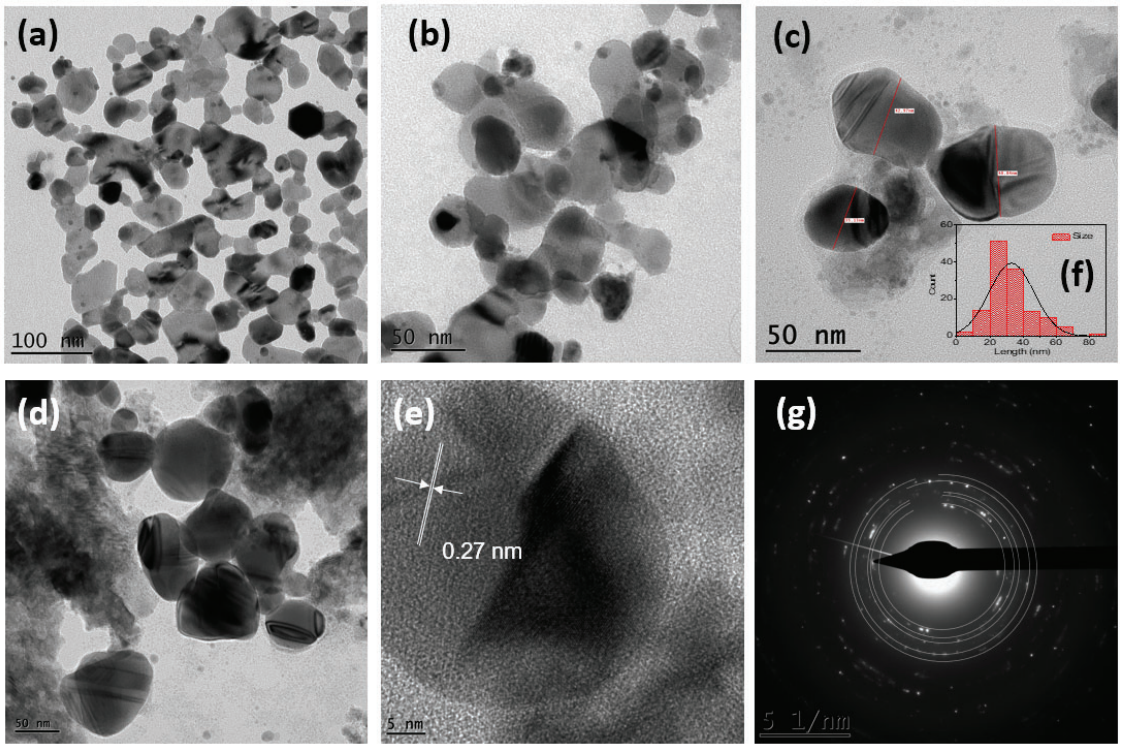

Figure 4. *Transmission electron micrographs of the Ag-ZnO showing: (a-d) the typical morphology of the powder at nanoscale, (e) high-resolution image of the individual nanoparticles, (g) selected area electron diffraction pattern, and (f) the size distribution histogram.*

Figure 5 shows the optical transmittance of Ag-ZnO/Water nanofluid with four mass fractions: 50 ppm, 30 ppm, 15 ppm, and 5 ppm. As the concentration of Ag-ZnO increases from 5 to 50 ppm in the nanofluid, the transmittance in the UV region of the spectrum decreases. The effect of the mass fraction of the nanofluid is found to be insignificant in the 400–1100 nm range. The majority of spectral energy between 400 nm and 1100 nm can pass through the Ag-ZnO /water nanofluid, while the remaining energy is absorbed. As a result of this nanofluid's ability to absorb spectral energy that is not used by the solar cell, heat harvesting has improved. Therefore, it may be regarded as a suitable optical nanofluid for PV-T systems that use spectral splitting, as the working area of PV/T systems is reported to be between 400 nm and 1200 nm.

ZnO has a wide bandgap of nearly 3.3 eV in bulk. In nanoscale morphologies this may increase slightly depending on the size, shape, etc. Because of this band gap, the absorption edge of ZnO is 3.3 eV which corresponds to about 375 nm [24]. Therefore, ZnO absorbs significantly in the UV region and the peak is observed near band edges that decreases gradually on either side. ZnO may be completely transparent in the wavelength below 400 nm if there exist no energy states within the gap [23]. These gap states usually arise because of donors for n-type (or acceptors for p-type) which lie just below the conduction band (or above valence band for p-type). ZnO shows intrinsically n-type character due to unintentionally doped oxygen vacancies and zinc interstitials [21, 25]. These crystal defects have low formation energies in the ZnO lattice and hence readily nucleate. Zinc interstitial (Zni) lies just below conduction band whereas oxygen vacancies depending on their charged state can lie shallow or deep within the gap. These states are referred to as gap states and they may lead to photo-absorption and emission of energies equivalent to the difference between the defect state and the valence band maximum. Therefore, they may increase the visible emission as their energies are 1-2 eV above valence band maxima.

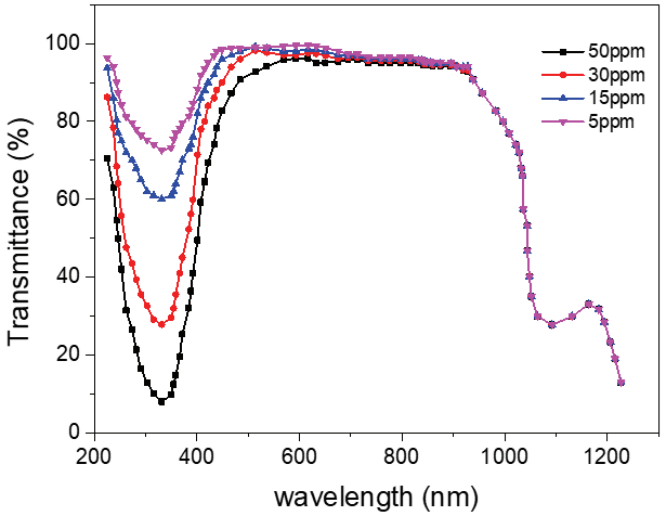

Figure 5. *UV-visible transmittance spectra of the Ag-ZnO nanoparticles at different dilutions in water.*

On the other hand, the silver lattice may show significant absorption that is usually caused in noble metals due to presence of surface plasmon resonance (SPR). The SPR is called collective oscillations of the free electron in metals which is the result of excitation due to electromagnetic radiation of appropriate energy (frequency); For Silver, this absorption mostly occurs at about 400 nm. Therefore, the corresponding amount of energy is called the plasmon absorption energy. In this case, the work function of Ag (fermi level is only slightly smaller than that of ZnO). Thus, any electron excited to a virtual SPR level is higher in energy that conduction band of ZnO and hence the charge transfer from Ag to ZnO is highly likely. This configuration of Ag-ZnO not only allows the absorption of near UV regions but may also result in visible emission as the charges transferred to ZnO may undergo a radiative transition and emit photons of smaller energy which happens to be in the visible region. Thus, this offers a win-win situation where the Ag absorbs the near UV and ZnO emits the visible light. This Additional visible light emitted can be beneficial to the PV sell and enhance the efficiency.

Conclusions

In this paper, results were presented relating to the use of Ag-ZnO nanofluids (nanoparticles suspended in water as the base fluid) for spectral-splitting PV-T applications. Ag-ZnO nanoparticles were synthesised by the solvothermal method. Several characterization techniques were utilised, including electron microscopy, X-ray diffraction and Raman spectroscopy. The XRD patterns revealed that Ag may coexist with the ZnO nanoparticles and these may have poor crystalline nature. The presence of Ag has also been confirmed by energy dispersive spectroscopy. The optical properties of the proposed nanofluids were investigated over a range of concentrations. The nanofluids exhibited a high degree of spectral selectivity, in the UV and IR regions which were absorbed or reflected respectively. In the visible region, a good transmittance was observed, which promotes higher PV cell efficiencies. In future work, visual inspection and dynamic light scattering techniques will be applied to evaluate the long-term stability of these nanofluids.

Acknowledgments

This work was supported by the Marie Skłodowska-Curie Individual Fellowships under the European Union's Horizon 2020 research and innovation program, grant agreement no. 101028904 — NANOSPLIT — H2020-MSCA-IF-2020. The authors are thankful to the central instrumentation facility of IISER Thiruvananthapuram for access to various characterization facilities. This work was also supported by the UK Engineering and Physical Sciences Research Council (EPSRC) [grant numbers EP/M025012/1, and EP/R045518/1] and by the Royal Society under an International Collaboration Award 2020 [grant number ICA\R1\201302]. The authors would like to thank UK company Solar Flow Ltd. (www.solar-flow.co.uk). Data supporting this publication can be obtained on request from cep-lab@imperial.ac.uk. For the purpose of Open Access, the authors have applied a CC BY public copyright licence to any Author Accepted Manuscript version arising from this submission.

References

[1] Al-Shohani W.A.M., Al-Dadah R., Mahmoud S., Reducing the thermal load of a photovoltaic module through an optical water filter. Appl Therm Eng 2016;109:475–486.

[2] Chow T.T., A review on photovoltaic/thermal hybrid solar technology. Appl Energy 2010;87:365–379.

https://doi.org/10.52202/069564-0158

[3] Candadai A.A., Kumar V.P., Barshilia H.C., Performance evaluation of a natural convective-cooled concentration solar thermoelectric generator coupled with a spectrally selective high temperature absorber coating. Solar Energy Materials and Solar Cells 2016;P3:333–341.

[4] Huang G., Curt S.R., Wang K., et al., Challenges and opportunities for nanomaterials in spectral splitting for high-performance hybrid solar photovoltaic-thermal applications: A review. Nano Materials Science 2020;2:183–203.

[5] Hong W., Li B., Li H., et al., Recent progress in thermal energy recovery from the decoupled photovoltaic/thermal system equipped with spectral splitters. Renewable and Sustainable Energy Reviews 2022;167:112824.

[6] Zachariah R., Amalnath V.N., Feasibility Study of Liquid-Based Spectral Beam Splitting Technique for Solar Panel Cooling. 2020;3–18.

[7] Abdelrazik A.S., The potential of liquid-based spectrally-selective optical filtration and its use in hybrid photovoltaic/thermal solar systems. Solar Energy 2023;249:569–605.

[8] Stanley C., Mojiri A., Rosengarten G., Spectral light management for solar energy conversion systems. Nanophotonics 2016;5:161–179.

[9] Hjerrild N.E., Crisostomo F., Chin R.L., et al., Experimental Results for Tailored Spectrum Splitting Metallic Nanofluids for c-Si, GaAs, and Ge Solar Cells. IEEE J Photovolt 2019;9:385–390.

[10] Zhang C., Shen C., Zhang Y., et al., Optimization of the electricity/heat production of a PV/T system based on spectral splitting with Ag nanofluid. Renew Energy 2021;180:30–39.

[11] Han X., Chen X., Wang Q., et al., Investigation of CoSO4-based Ag nanofluids as spectral beam splitters for hybrid PV/T applications. Solar Energy 2019;177:387–394.

[12] Abdelrazik A.S., Tan K.H., Aslfattahi N., et al., Optical properties and stability of water-based nanofluids mixed with reduced graphene oxide decorated with silver and energy performance investigation in hybrid photovoltaic/thermal solar systems. Int J Energy Res 2020;44:11487–11508.

[13] Huaxu L., Fuqiang W., Dong L., et al., Optical properties and transmittances of ZnO-containing nanofluids in spectral splitting photovoltaic/thermal systems. Int J Heat Mass Transf 2019;128:668–678.

[14] Huaxu L., Fuqiang W., Dong Z., et al., Experimental investigation of cost-effective ZnO nanofluid based spectral splitting CPV/T system. Energy 2020;194:116913.

[15] Khan M., Wei C., Chen M., et al., CTAB-mediated synthesis and characterization of ZnO/Ag core–shell nanocomposites. J Alloys Compd 2014;612:306–314.

[16] Barewar S.D., Chougule S.S., Heat transfer characteristics and boiling heat transfer performance of novel Ag/ZnO hybrid nanofluid using free surface jet impingement. Experimental Heat Transfer 2021;34:531–546.

[17] Barewar S.D., Tawri S., Chougule S.S., Experimental investigation of thermal conductivity and its ANN modeling for glycol-based Ag/ZnO hybrid nanofluids with low concentration. J Therm Anal Calorim 2020;139:1779–1790.

[18] Barewar S.D., Chougule S.S., Jadhav J., et al., Synthesis and thermo-physical properties of water-based novel Ag/ZnO hybrid nanofluids. J Therm Anal Calorim 2018;134:1493–1504.

[19] Biswas S., Ram S., Morphology and stability in a half-metallic ferromagnetic CrO2 compound of nanoparticles synthesized via a polymer precursor. Chem Phys 2004;306:163–169.

[20] Biswas S., Ram S., Synthesis of shape-controlled ferromagnetic CrO2 nanoparticles by reaction in micelles of Cr6+–PVA polymer chelates. Mater Chem Phys 2006;100:6–9.

[21] Biswas S., Singh S., Singh S., et al., Selective Enhancement in Phonon Scattering Leads to a High Thermoelectric Figure-of-Merit in Graphene Oxide-Encapsulated ZnO Nanocomposites. ACS Appl Mater Interfaces 2021;13:23771–23786.

[22] Song Y., Zhang S., Zhang C., et al., Raman Spectra and Microstructure of Zinc Oxide irradiated with Swift Heavy Ion. Crystals 2019;9:395.

[23] Srinatha N., No Y.S., Kamble V.B., et al., Effect of RF power on the structural, optical and gas sensing properties of RF-sputtered Al doped ZnO thin films. RSC Adv 2016;6:9779–9788.

[24] Urs K.M.B., Kamble V., Surface photovoltage response of zinc oxide microrods on prismatic planes: effect of UV, temperature and oxygen ambience. Journal of Materials Science: Materials in Electronics 2021;32:6414–6424.

[25] Xu PS, Sun YM, Shi CS, et al. The electronic structure and spectral properties of ZnO and its defects. Nucl Instrum Methods Phys Res B 2003; 199: 286–290.